

Influence of IMF draping direction and crustal magnetic field location on Martian ion beams

E. Carlsson^{a,b,c,*}, D. Brain^c, J. Luhmann^c, S. Barabash^a, A. Grigoriev^a,
H. Nilsson^a, R. Lundin^a

^aSwedish Institute of Space Physics, Box 812, SE-981 28 Kiruna, Sweden

^bDepartment of Physics, Luleå University of Technology, SE-971 87 Luleå, Sweden

^cSpace Sciences Laboratory, University of California at Berkeley, Berkeley, CA 94720-7450, USA

Accepted 30 October 2007

Available online 19 January 2008

Abstract

Data from the Ion Mass Analyzer (IMA) sensor of the ASPERA-3 instrument suite onboard Mars Express and data from the Magnetometer/Electron Reflectometer (MAG/ER) on Mars Global Surveyor have been analyzed to determine whether ion beam events (IBEs) are correlated with the direction of the draped interplanetary magnetic field (IMF) or the proximity of strong crustal magnetic fields to the subsolar point. We examined 150 IBEs and found that they are organized by IMF draping direction. However, no clear dependence on the subsolar longitude of the strongest magnetic anomaly is evident, making it uncertain whether crustal magnetic fields have an effect on the formation of the beams. We also examined data from the IMA sensor of the ASPERA-4 instrument suite on Venus Express and found that IBEs are observed at Venus as well, which indicates the morphology of the Martian and Venusian magnetotails are similar.

© 2008 Published by Elsevier Ltd.

Keywords: Solar wind erosion; Escape; Ion beams; IMF

1. Introduction

In a previous study by Carlsson et al. (2006) the composition of the escaping ion beam events (IBEs) observed at Mars by the ASPERA-3 instrument (Barabash et al., 2004) on Mars Express (MEX) was analyzed. The results showed that the flux ratios of CO_2^+/O^+ and O_2^+/O^+ are 0.9 and 0.2, respectively, for the time period 23 April 2004–31 December 2004, during the declining phase of the recent solar cycle. Two types of ion populations are observed by ASPERA-3 in the Martian wake, where one population appears as a spatially diffuse flux over a broad energy range and the other consists of IBEs. The count rates of the IBEs exceed the normal, widely distributed background of ions by a factor of at least 50 and normally

by 100. They are distributed in narrow angular ranges (beamed). Furthermore, IBEs in the wake appear in a narrow energy band, normally from 700 to 900 eV. In this paper we present a supplemental study of IBEs and their correlation to the magnetic field draping and crustal magnetic fields. Fedorov et al. (2006) and Barabash et al. (2007) show that there is a clear correlation between the convection electric field and the escape of all Martian planetary ions measured with ASPERA-3 with energies ranging from 30 eV to 30 keV, where the ions are lost preferably in the hemisphere in the direction of the electric field. However, these analyses did not distinguish between the IBEs and the distributed background ions. Here we investigate whether the two types of ions behave differently, suggesting a different acceleration process for the IBEs, or the same.

Due to the absence of an intrinsic magnetic field, the solar wind can penetrate deep into the Martian upper atmosphere (270 km) and cause atmospheric erosion

*Corresponding author at: Swedish Institute of Space Physics, Box 812, SE-981 28 Kiruna, Sweden. Tel.: +46 980 79124; fax: +46 980 79050.

E-mail address: ella@irf.se (E. Carlsson).

(Lundin et al., 2004). There are numerous ways which allow ions to escape from Mars (e.g., Luhmann and Bauer, 1992, and references therein); such as thermal escape (Jeans), ion pick-up, sputtering, ion outflow from cusps (Krymskii et al., 2002; Lundin et al., 2006) and bulk plasma removal (e.g., detached ionospheric clouds caused by Kelvin–Helmoltz instabilities, Wolff et al., 1980). When neutrals in the upper atmosphere of Mars become ionized by photons, electrons or by charge exchange, they become affected by the frozen-in interplanetary magnetic field (IMF) and can be picked up by the solar wind and accelerate, while gyrating, in the direction of the convection electric field of the solar wind. The IMF is related to the solar wind convection electric field by

$$\vec{E}_{\text{sw}} = -\vec{v}_{\text{sw}} \times \vec{B} \quad (1)$$

so that the IMF direction determines the direction of the \vec{E}_{sw} .

The solar wind interaction with Mars has been investigated by numerous authors since the first probe (Mars-2) reached Mars in 1971 (Vaisberg, 1992, and references therein). The morphology of the Martian tail has been studied in detail starting with Phobos-2 (e.g., Lundin et al., 1990), which characterized the energy and composition of the escaping constituents. Fedorov et al. (2006) made statistical studies of the Martian magnetotail where they identified two populations of ions. One of these regimes was observed in the planetary shadow where planetary (heavy) ions had been accelerated to the energy of solar wind protons. The other regime of ions is also of planetary origin, however, these ions are accelerated to an energy >2 keV, which decreases as the ions approach the plasma sheet. Beams, or tail rays, in the wake of Venus were first described by Brace et al. (1987) as electron enhancements which were thought to be part of a sheet like ionospheric plasma structure. Ong et al. (1991) identified tail rays in the Venusian wake and studied their density, distribution and spatial extent where they came to the conclusion that the rays were filaments of ionospheric plasma which extended downstream from the night side ionosphere. Comparative studies of the Martian and Venusian wakes have been conducted (Dubinin et al., 1991), where notable similarities have been pointed out, such as beams of O^+ .

We investigate the IBEs of Mars in order to understand their importance and relevance in the total outflow of ions and the possible impact they could have had on the past climate. The results from this study could also be applicable and helpful in the analysis of the solar wind interaction with other planets, e.g., Venus.

The controversial question regarding the existence of a past dense Martian atmosphere is yet unresolved. The ancient outflow channels (Malin and Edgett, 2003) suggest a somewhat warmer and wetter Mars, when the atmosphere must have been more substantial (Kasting, 1991) in order for water to remain in a stable and liquid form on the

surface. Pre-Hesperian impactors (Melosh and Vickery, 1989) and carbonate reservoirs in the strata (Huguenin, 1975) have been proposed as plausible sink channels for the lost atmosphere. Another possible sink channel is the solar wind erosion of the Martian atmosphere where the investigation of escaping ions is important. Barabash et al. (2007) report that the present escape rates of O^+ , O_2^+ and CO_2^+ observed on MEX are as low as 1.6×10^{23} , 1.5×10^{23} and $8 \times 10^{22} \text{ s}^{-1}$, respectively. These values are a factor of 100 lower than those reported from Phobos-2 (Lundin et al., 1990), and too low to account for a past dense atmosphere of the kind needed to explain the water-related features. However, extrapolation of these escape numbers over the past 4 Gy is complicated by the uncertain time history of solar wind variations as well as instrument and spatial distribution uncertainties. Moreover, the observed escape rates were determined from a period of low solar activity. Even if these rates were erroneous with a factor of 100, the total escape of CO_2^+ and the constituents of H_2O by ion escape alone could not have been more than 4 mbar and a few cm, respectively, for the past 3.5 Gy (Barabash et al., 2007).

In this study we combine the data from the Ion Mass Analyzer (IMA) (Barabash et al., 2004) onboard MEX with IMF proxy information derived from the Magnetometer/Electron Reflectometer (MAG/ER) (Acuña et al., 2001) on Mars Global Surveyor (MGS), in order to determine if the solar wind convection electric field controls the IBEs in the same way that it controls the more general pick up ion population. Section 2 is devoted to the methodology. The results are presented in Section 3 followed by a discussion in Section 4 and a summary in Section 5.

2. Methodology

First we analyzed data from the ASPERA-3 IMA sensor in order to find clear planetary ion events. The IMA sensor operates in the energy range of $0.03\text{--}32 \text{ keV}/q$ and is capable of detecting H^+ , He^{2+} , O^+ and molecular ions within the range of $20 < M/q < 80$ (Barabash et al., 2004). Electrostatic sweeping provides the sensor with a $\pm 45^\circ$ polar angle response, which gives the instrument an intrinsic field of view (FOV) of $90^\circ \times 360^\circ$. The FOV is divided into 16 (5.6° each) polar angles and 16 (22.5° each) azimuth sectors. The top-hat electrostatic analyzer (ESA) selects ions by energy, with an energy resolution of 8%, which then enter the mass selection and detection unit. Permanent magnets then deflect the ions along different trajectories, depending on their mass and charge. The magnetic assembly can be biased with a post-acceleration up to 4.2 kV. In a mode without any post-acceleration, the sensor has the highest mass resolution but lighter particles with low energies, such as H^+ , are deflected in their flight paths to such an extent that they miss the micro-channel plate (MCP) altogether and cannot be detected. Post-acceleration up to 4.2 keV allows the detection of protons

(for solar wind observations). However, this limits the mass resolution. After passing the magnet assembly the ions hit the position sensitive anode composed of the 16 sectors \times 32 rings, which determines both the azimuth (sector) and mass per charge of the incoming ion species.

To avoid the backgrounds induced by strong proton fluxes in the magnetosheath, which can cause ghost counts in the IMA sensor due to contamination of adjacent mass channels, we only examined orbits inside the induced magnetosphere boundary (IMB) as seen in Fig. 1(a). We examined all orbits of MEX starting from 23 April 2004 to 3 March 2005 and found 150 clear IBEs, which are presented in the figure. The orbits are displayed in cylindrical MSO coordinates expressed in Mars radii, R_M . The z -axis in this coordinate system is directed northward, perpendicular to the ecliptic plane, the x -axis

is directed toward the Sun with the center of Mars as its origin and the y -axis completes the right-handed system. The vertical axis $R = \sqrt{y^2 + z^2}$ in the figure represents the distance from the satellite to the Mars–Sun line. The bow shock and the IMB in the figure are derived by using analytical fits derived by Kallio (1996). The drifting orbit of MEX is highly elliptical with an inclination of 86° and an orbit period of 6.7 h. Fig. 1(b) shows the number of passes by MEX, through the region studied here when the IMA sensor had a post-acceleration of 2.4 kV. (This was one of the boundary conditions for the previous study of the IBEs by Carlsson et al., 2006, where a fitting program was used to extract the masses for heavy ion components.) It thus represents the orbital coverage for the present study.

The IBEs often appear in just a couple of azimuth sectors or less, as seen in Fig. 2. This particular beam

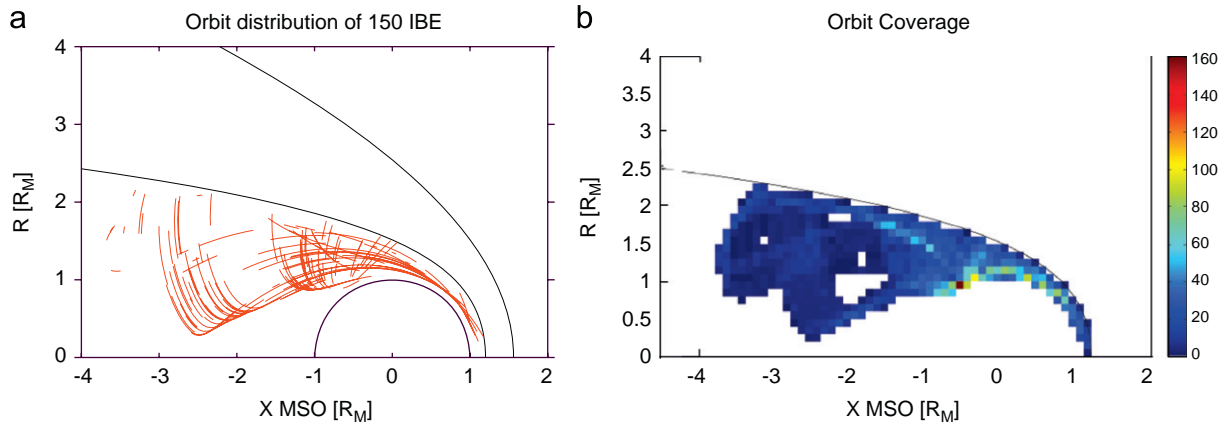


Fig. 1. (a) shows parts of the orbits that correspond to the time intervals of the 150 IBEs used in this study. The orbits are displayed in cylindrical MSO coordinates. The position of the bow shock and the induced magnetosphere boundary are also shown (Kallio, 1996). (b) shows the number of times Mars Express sampled certain spatial bins inside the induced magnetosphere boundary when the IMA sensor had a post-acceleration of 2.4 kV.

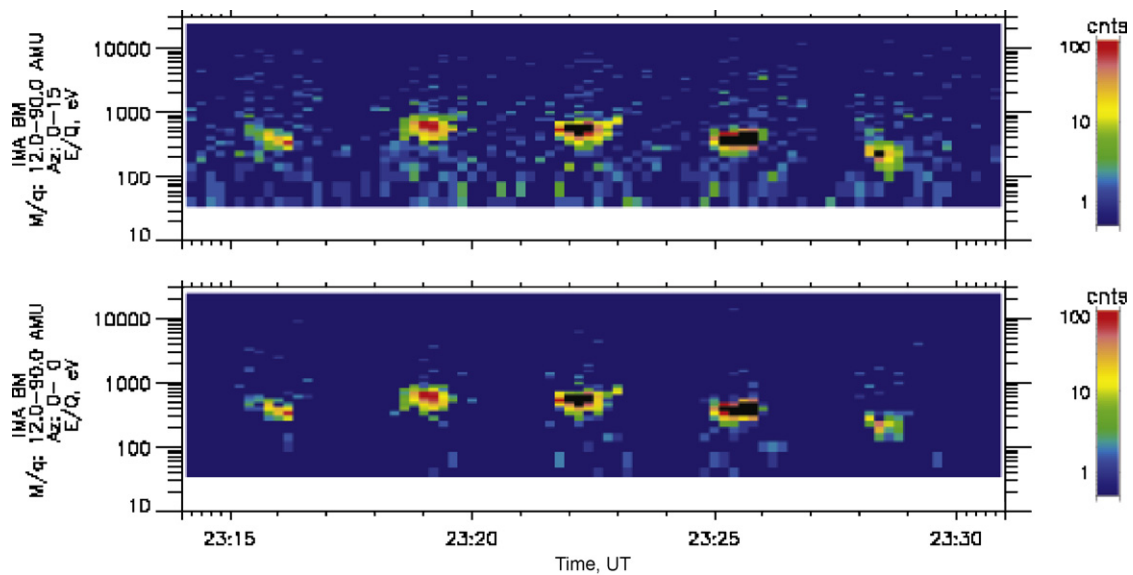


Fig. 2. The figure shows an ion beam event which occurred 27 February 2005 at 23.15 UT and lasted for approximately 15 min. The y -axis shows the energy range (eV), the x -axis the time (UT) and the count rate is color coded. Normally the IBEs have count rates a factor of 100 higher than normal background inside the induced magnetosphere boundary (black color in the figure represents a count rate > 100). In the top panel we have integrated the count rate of the ion beam event overall 16 azimuth angles and in the bottom panel only over one angle.

occurred 27 February 2005 at 23.15 UT and lasted for approximately 15 min and was observed in the Martian tail. Normally the IBEs have higher count rates by a factor of 100 than normal background counts inside the IMB. In the top panel we have integrated the count rate of the IBE overall 16 azimuth sectors and 16 polar angles and in the bottom panel only over one sector (and over 16 polar angles). This shows that the IBEs are very narrow spatially and hence beams. The energy band is also quite narrow for the IBEs (here approximately 200–700 eV).

The IMF draping directions were derived from the MAG/ER sensor in a study by Brain et al. (2006). The azimuth directions of the draped magnetic field were derived for each spacecraft orbit at the day side between 50°N and 60°N latitude, a band which lacks significant crustal magnetic fields which could influence the draping direction. MGS had a polar and circular orbit fixed in local time at 2 am/2 pm with an orbital period of nearly 2 h. The median value for the IMF direction was calculated for each orbit within the latitude band mentioned above for which it took approximately 3.3 min for MGS to pass. Since the recorded IMF draping direction rarely occurred at the same time as the IBEs, the closest corresponding IMF direction was chosen, which inserts a time delay of maximum 1 h between the IBEs and the correlating IMF draping direction. The Y_{MSO} and Z_{MSO} coordinates of the IBEs were then rotated by their corresponding IMF draping direction by

$$Y_{\text{MSE}} = Y_{\text{MSO}} \cos \alpha + Z_{\text{MSO}} \sin \alpha, \quad (2)$$

$$Z_{\text{MSE}} = -Y_{\text{MSO}} \sin \alpha + Z_{\text{MSO}} \cos \alpha, \quad (3)$$

where α is the correlating IMF draping direction (0° in the local eastward direction and 90° in the local northward

direction of the MGS). By this rotating procedure the IBEs were organized by the IMF draping direction.

3. Results

Fig. 3(a) shows the locations of the IBEs in MSO coordinates (as viewed from the Sun) and Fig. 3(b) shows the IBE locations in a MSE frame where $X_{\text{MSO}} = X_{\text{MSE}}$ and Z_{MSE} is aligned with the plane of the convection electric field of the solar wind. We assume that the IMF draping direction in the subsolar region sampled by MGS in its orbit at ~400 km altitude is directly correlated with the upstream IMF clock angle, such that: $Y_{\text{IMF}} \approx Y_{\text{MSE}}$ and $Z_{\text{IMF}} \approx Z_{\text{MSE}}$ (Brain et al., 2006) (see discussion in Section 4).

Earlier studies (Fedorov et al., 2006; Barabash et al., 2007) show that the overall ion escape observed on MEX is related to the direction of the electric field, where ions are accelerated in the direction of this field and lost. In Fig. 3(b) it appears that most of the IBEs are detected in the northern hemisphere of Mars in the MSE coordinate system, toward which the electric field is pointing. This result is consistent with the previous studies of all of the ions. There is also a suggestion of an alignment of the beams parallel to the electric field (south–north).

We also investigated the dependence on the subsolar longitude to see whether the IBEs are associated with the position of crustal magnetic fields (Acuña et al., 1999) with respect of the Sun. Since it takes approximately 1.5 min for an O^+ (1000 eV) to reach the tail of Mars ($x = -1R_{\text{M}}$), we can assume that the planetary longitude of the subsolar point at the time of the IBEs represents the prevailing conditions with a time delay of less than 2 min. Fig. 4 shows that, within uncertainties, there appears to be no

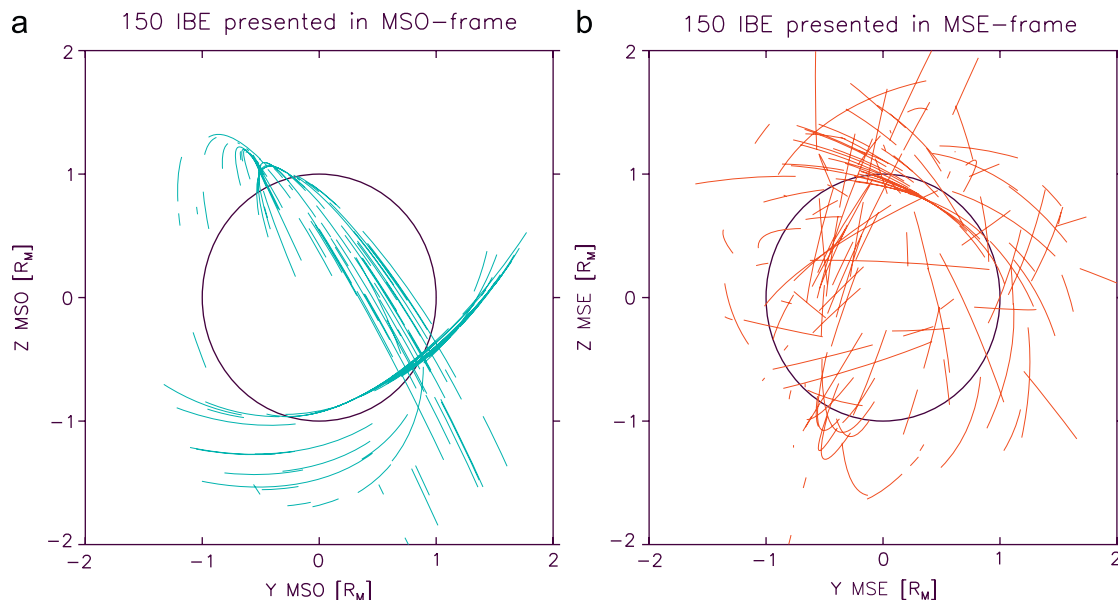


Fig. 3. (a) shows MEX location during the 150 IBEs in MSO coordinates and (b) in MSE coordinates where the solar wind convection electric field points upward.

clear correlation between subsolar longitude and the observation of IBEs. This is consistent with the result of Nilsson et al. (2006), who shows that the IBEs are not more commonly observed above crustal magnetic fields. The strongest crustal fields can be found at a subsolar longitude of 180°. An increase in IBE frequency can be seen here, but also at 60–75°, 90–105°, 150–165° and a small peak at 275–300°. However, a clear decrease in the IBE frequency can be found for subsolar longitudes of 0–30°, when the strongest crustal fields are located near midnight.

4. Discussion

To verify our technique we have also used the same method of extracting the IMF directions used by Fedorov et al. (2006), which used MGS data recorded when: (1) the solar-zenith angle was less than 60° and (2) where Cain’s model (Cain et al., 2003) predicts a crustal magnetic field less than 3 nT in magnitude. For conditions where (1) and (2) were true, the following IMF clock angle calculation

was performed:

$$\theta = \arctan(B_{z\text{MSO}}/B_{y\text{MSO}}). \tag{4}$$

We then used these IMF directions and confirmed the results from Fig. 3(b).

It must also be noted that the IMF draping direction can change rapidly and on any timescale, which leaves an uncertainty since it can change at any time during one MGS orbit. Contributions of magnetic fields generated by ionospheric currents can also result in erroneous IMF directions (“weathervaning”, e.g., see Brain et al., 2006), which we estimate to be approximately 45° from the nominal IMF direction. Furthermore, the change of solar longitude causes Mars to wobble, which can cause changes of ±25° in the IMF draping direction. Despite these uncertainties we still obtained a north–south trend in Fig. 3(b), and found more occurrences of IBEs in the northern MSE hemisphere. The results suggest that the IBEs are accelerated in the direction of the solar wind convection electric field and lost over one hemisphere in a manner described several decades ago for Venus by Cloutier et al. (1969).

In Fig. 4 it appears that the IBEs are evenly spread over almost all subsolar longitudes. However, there is an apparent decrease of IBE frequency for subsolar longitudes of 0°, when the strong magnetic crustal fields are near midnight. This result is in contrast to the increase that would occur if the ions in these beams escaped preferentially on the night side via cusps created by the stronger magnetic fields in the Martian crust (Lundin et al., 2006). The decrease in ion beams when the strong fields are in the deep wake might be due to some inhibition of antisunward ion flows by their presence there. Since Mars lacks an intrinsic magnetic field, the solar wind penetrates the upper atmosphere of Mars. When the IMF penetrates deep enough at the subsolar point, it could reconnect with the magnetic anomalies and facilitate the escape of planetary heavy ions via open field lines in cusps, which could explain the increase at subsolar longitude close to 180°.

We next examined ASPERA-4 observations from Venus Express to determine whether similar IBEs can be found at

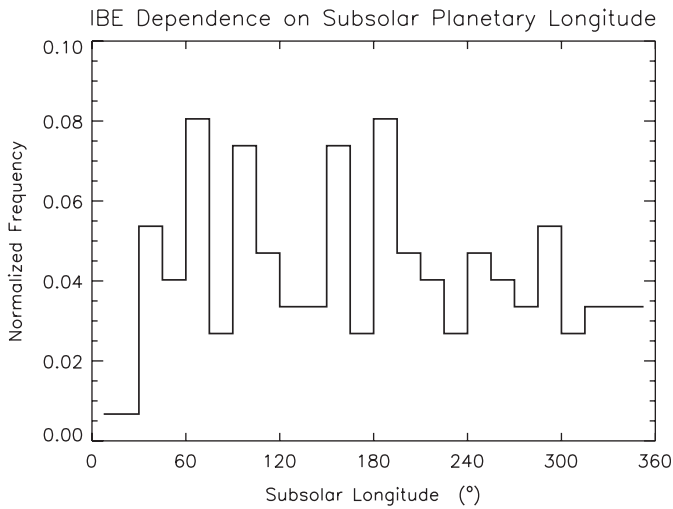


Fig. 4. The figure shows a histogram of the planetary subsolar longitude at the time of each IBE in bins of 15°. The strongest crustal magnetic field can be found at 180°.

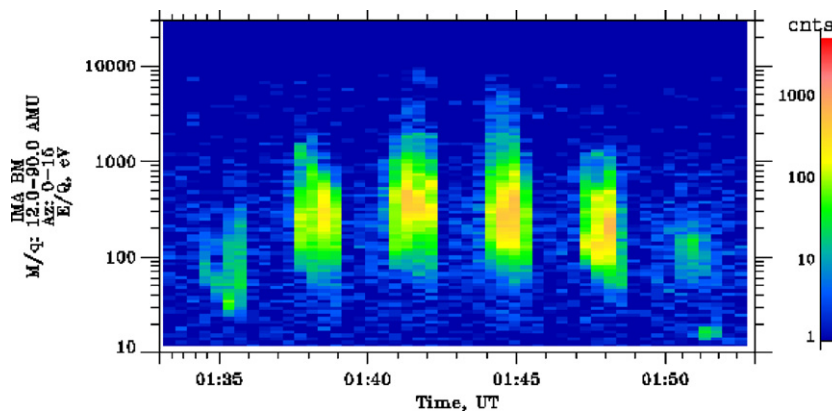


Fig. 5. An ion beam event found in the Venusian tail which displays similar IBEs characteristics as the Martian IMBs.

Venus. By analyzing data from the ASPERA-4 IMA sensor we found several cases that were similar to the ones found at Mars. Fig. 5 shows an IBE found in the Venusian tail which displays similar characteristics to those at Mars. The IBEs on Venus have similar energy ranges to those at Mars and are spatially distributed in similar manner, which could imply that the IBEs at Venus form and evolve in the same way as on Mars. This particular event found on the night side is shaped as an inverted V, which was first detected at Mars by the satellite Phobos-2 (Lundin et al., 1989). Inverted Vs are characterized by narrow beams of oppositely directed ions and electrons and have been compared to ion outflows in Earth's auroral zone (Lundin et al., 2006). The important point of this observation at Venus, however, is that crustal magnetic fields are evidently not necessary to produce ion beams.

The detection of very low energy ions ($E < 30$ eV) is unfortunately beyond the capability of the IMA sensor. These cold and still undetected ions could comprise major parts of the escaping ion population. Phobos-2 could measure ions down to energy levels of 0.5 eV. However, Phobos-2 did not have a satellite potential control which could have affected the measurements. Modeling that is based on the MEX measurements of the IBEs and other escaping ions can perhaps fill the gaps of knowledge in these unobserved energy ranges and motivate future instrument design for Mars missions.

5. Conclusions and future studies

This paper is a continuation of the analysis of IBEs reported by Carlsson et al. (2006). We investigate whether the IBEs are correlated with the draping direction of the IMF, which would indicate that the beams are affected and perhaps accelerated by the convection electric field of the solar wind. A dependence between the draping direction of the IMF and the IBEs was detected, where the beams are moderately aligned in the direction of the E-field and most of them are clustered in the hemisphere toward which the E-field points. We also investigated whether the IBEs showed dependence with subsolar longitude, which would indicate that they may be affected by crustal magnetic fields. We detected no clear correlation between subsolar longitude and the frequency of observation of IBEs, and hence the position of the strongest magnetic anomaly with respect to the solar wind flow does not appear to play an important part in their formation. We report that IBEs are present at Venus and are generally similar to those observed at Mars, both with regard to energy range and spatial distribution. This then suggests that the physics of the ion beam source is similar at both planets (also that crustal sources are not required for their creation). Our future efforts will investigate whether different characteristics of IBEs (such as peak energy, composition, direction) are influenced by these drivers. We will also examine whether solar wind pressure and solar activity influence IBE observations. Such studies, using hundreds of addi-

tional IBEs identified in ASPERA-3 and ASPERA-4 data, will help to uncover how ion beams form and their importance in the total outflow of ions from the atmospheres of Mars and Venus.

Acknowledgments

Ella Carlsson thanks the Swedish National Graduate School of Space Technology, the Swedish National Space Board and the Kempe Foundations for financial support.

References

- Acuña, M.H., Connerney, J.E.P., Ness, N.F., Lin, R.P., Mitchell, D., Carlson, C.W., McFadden, J., Anderson, K.A., Rème, H., Mazelle, C., Vignes, D., Wasilewski, P., Cloutier, P., 1999. Global distribution of crustal magnetization discovered by the Mars Global Surveyor MAG/ER experiment. *Science* 284 (5415), 790–793.
- Acuña, M.H., Connerney, J.E.P., Wasilewski, P., Lin, R.P., Mitchell, D., Anderson, K.A., Carlson, C.W., McFadden, J., Rème, H., Mazelle, C., Vignes, D., Bauer, S.J., Cloutier, P., Ness, N.F., 2001. Magnetic field of Mars: summary of results from the aerobraking and mapping orbits. *J. Geophys. Res.* 106 (E10), 23403–23418.
- Barabash, S., Lundin, R., Andersson, H., Gimholt, J., Holmström, M., Norberg, O., Yamuchi, M., Asamura, K., Coates, A., Linder, D.R., Kataria, D.O., Curtis, C.C., Hsieh, K.C., Sandel, B.R., Fedorov, A., Grigoriev, A., Budnik, E., Grande, M., Carter, M., Reading, D.H., Koskinen, H., Kallio, E., Riihela, P., Säles, T., Kozyra, J., Krupp, N., Livi, S., Woch, J., Luhmann, J., McKenna-Lawlor, S., Orsini, S., Cerulli-Irelli, R., Maggi, M., Morbidini, A., Mura, A., Milillo, A., Roelof, E., Williams, D., Sauvaud, J.-A., Thocaven, J.-J., Moreau, T., Winningham, D., Frahm, R., Scherrer, J., Sharber, J., Wurz, P., Bolchsler, P., 2004. ASPERA-3: analyser of space plasmas and energetic ions for Mars Express. *ESA Special Publication SP-1240*, 121–139.
- Barabash, S., Fedorov, A., Lundin, R., Sauvaud, J.-A., 2007. Martian atmospheric erosion rates. *Science* 315 (5811), 501–503.
- Brace, L.H., Kasprzak, W.T., Taylor, H.A., Theis, R.F., Russell, C.T., Barnes, A., Mihalov, J.D., Hunten, D.M., 1987. The ionotail of Venus—its configuration and evidence for ion escape. *J. Geophys. Res.* 92, 15–26.
- Brain, D., Mitchell, D., Halekas, J., 2006. The magnetic field draping direction at Mars from April 1999 through August 2004. *Icarus* 182 (2), 464–473.
- Cain, J.C., Ferguson, B.B., Mozzoni, D., 2003. An $n = 90$ internal potential function of the Martian crustal magnetic field. *J. Geophys. Res.* 108 (E2), 5008.
- Carlsson, E., Fedorov, A., Barabash, S., Budnik, E., Grigoriev, A., Gunell, H., Nilsson, H., Sauvaud, J.-A., Lundin, R., Futaana, Y., Holmström, M., Andersson, H., Yamauchi, M., Winningham, J.D., Frahm, R.A., Sharber, J.R., Scherrer, J., Coates, A.J., Linder, D.R., Kataria, D.O., Kallio, E., Koskinen, H., Säles, T., Riihela, P., Schmidt, W., Kozyra, J., Luhmann, J., Roelof, E., Williams, D., Livi, S., Curtis, C.C., Hsieh, K.C., Sandel, B.R., Grande, M., Carter, M., Thocaven, J.-J., McKenna-Lawlor, S., Orsini, S., Cerulli-Irelli, R., Maggi, M., Wurz, P., Bolchsler, P., Krupp, N., Woch, J., Fränz, M., Asamura, K., Dierker, C., 2006. Mass composition of the escaping plasma at Mars. *Icarus* 182 (2), 320–328.
- Cloutier, P.A., McElroy, M.B., Michel, F., 1969. Modification of the Martian ionosphere by the solar wind. *J. Geophys. Res.* 74 (26), 6215–6228.
- Dubinin, E., Lundin, R., Riedler, W., Schwingenschuh, K., Luhmann, J.G., 1991. Comparison of observed plasma and magnetic field structures in the wakes of Mars and Venus. *J. Geophys. Res.* 96, 11189–11197.

- Fedorov, A., Budnik, E., Sauvaud, J.-A., Mazelle, C., Barabash, S., Lundin, R., Acuña, M., Holmström, M., Grigoriev, A., Yamauchi, M., Andersson, H., Thocaven, J.-J., Winningham, D., Frahm, R., Sharber, J.R., Scherrer, J., Coates, A.J., Linder, D.R., Kataria, D.O., Kallio, E., Koskinen, H., Säles, T., Riihelä, P., Schmidt, W., Kozyra, J., Luhmann, J., Roelof, E., Williams, D., Livi, S., Curtis, C.C., Hsieh, K.C., Sandel, B.R., Grande, M., Carter, M., McKenna-Lawler, S., Orsini, S., Cerulli-Irelli, R., Maggi, M., Wurz, P., Bochsler, P., Krupp, N., Woch, J., Fränz, M., Asamura, K., Dierker, C., 2006. Structure of the Martian wake. *Icarus* 182 (2), 329–336.
- Huguenin, R.L., 1975. Mars: chemical weathering as a massive volatile sink. *Icarus* 28 (2), 203–212.
- Kallio, E., 1996. An empirical model of the solar wind flow around Mars. *J. Geophys. Res.* 101 (A5), 11133–11148.
- Kasting, J.F., 1991. O₂ condensation and the climate of early Mars. *Icarus* 94, 1–13.
- Krymskii, A.M., Breus, T.K., Ness, N.F., Acuña, M.H., Connerney, J.E.P., Crider, D.H., Mitchell, D.L., Bauer, S.J., 2002. Structure of the magnetic field fluxes connected with crustal magnetization and topside ionosphere at Mars. *J. Geophys. Res. (Space Physics)* 107 (A9), SIA 2–1, CiteID 1245, doi:10.1029/2001JA000239.
- Luhmann, J.G., Bauer, S.J., 1992. Solar wind effects on atmosphere evolution at Venus and Mars. In: *Venus and Mars: Atmospheres, Ionospheres, and Solar Wind Interactions. Proceedings of the Chapman Conference, Balatonfured, Hungary, June 4–8, 1990 (A92-50426 21-91)*. American Geophysical Union, Washington, DC, pp. 417–430.
- Lundin, R., Borg, H., Hultqvist, B., Zakharov, A., Pellinen, R., 1989. First measurements of the ionospheric plasma escape from Mars. *Nature* 341, 609–612.
- Lundin, R., Zakharov, A., Pellinen, R., Barabash, S., Borg, H., Dubinin, E., Hultqvist, B., Koskinen, H., Liede, I., Pissarenko, N., 1990. ASPERA/Phobos measurements of the ion outflow from the Martian ionosphere. *Geophys. Res. Lett.* 17, 873–876.
- Lundin, R., Barabash, S., Andersson, H., Holmström, M., Grigoriev, A., Yamauchi, M., Sauvaud, J.-A., Fedorov, A., Budnik, E., Thocaven, J.-J., Winningham, D., Frahm, R., Scherrer, J., Sharber, J., Asamura, K., Hayakawa, H., Coates, A., Linder, D.R., Curtis, C., Hsieh, K.C., Sandel, B.R., Grande, M., Carter, M., Reading, D.H., Koskinen, H., Kallio, E., Riihela, P., Schmidt, W., Säles, T., Kozyra, J., Krupp, N., Woch, J., Luhmann, J., McKenna-Lawler, S., Cerulli-Irelli, R., Orsini, S., Maggi, M., Mura, A., Milillo, A., Roelof, E., Williams, D., Livi, S., Brandt, P., Wurz, P., Bochsler, P., 2004. Solar wind-induced atmospheric erosion at Mars: first results from ASPERA-3 on Mars Express. *Science* 304 (5692), 1933–1936.
- Lundin, R., Winningham, D., Barabash, S., Frahm, R., Holmström, M., Sauvaud, J.-A., Fedorov, A., Asamura, K., Coates, A.J., Soobiah, Y., Hsieh, K.C., Grande, M., Koskinen, H., Kallio, E., Kozyra, J., Woch, J., Fraenz, M., Brain, D., Luhmann, J., McKenna-Lawler, S., Orsini, R.S., Brandt, P., Wurz, P., 2006. Plasma acceleration above Martian magnetic anomalies. *Science* 311 (5763), 980–983.
- Malin, M., Edgett, K., 2003. Evidence for persistent flow and aqueous sedimentation on early Mars. *Science* 302, 1931–1934.
- Melosh, H.J., Vickery, A.M., 1989. Impact erosion of the primordial atmosphere of Mars. *Nature* 338, 487–489.
- Nilsson, H., Carlsson, E., Gunell, H., Futaana, Y., Barabash, S., Lundin, R., Fedorov, A., Soobiah, Y., Coates, A., Fränz, M., Roussos, E., 2006. Investigation of the influence of magnetic anomalies on ion distributions at Mars. *Space Sci. Rev.* 126 (1–4), 355–372.
- Ong, M., Luhmann, J.G., Russell, C.T., Strangeway, R.J., Brace, L.H., 1991. Venus ionospheric tail rays—spatial distributions and interplanetary magnetic field control. *J. Geophys. Res.* 96, 17751–17761.
- Vaisberg, O.L., 1992. The solar wind interaction with Mars—a review of results from early Soviet missions to Mars. In: *Venus and Mars: Atmospheres, Ionospheres, and Solar Wind Interactions. Proceedings of the Chapman Conference, Balatonfured, Hungary, June 4–8, 1990 (A92-50426 21-91)*. American Geophysical Union, Washington, DC, pp. 311–326.
- Wolff, R.S., Goldstein, B.E., Yeates, C.M., 1980. The onset and development of Kelvin–Helmholtz instability at the Venus ionopause. *J. Geophys. Res.* 85, 7697–7707.